FRONTIERS OF PHYSICS

RESEARCH ARTICLE
Volume 17 / Issue 5 / 52507 / 2022

Nonreciprocal ground-state cooling of mechanical resonator in a spinning optomechanical system

Junya Yang, Chengsong Zhao, Zhen Yang, Rui Peng, Shilei Chao, Ling Zhou†

School of Physics, Dalian University of Technology, Dalian 116024,China
Corresponding author. E-mail: †zhlhxn@dlut.edu.cn
Received May 4, 2022; accepted August 18, 2022

ABSTRACT

We theoretically present a scheme for nonreciprocal ground-state cooling in a double-cavity spinning optomechanical system which is consisted of an optomechanical resonator and a spinning optical harmonic resonator with directional driving. The optical Sagnac effect generated by the whispering-gallery cavity (WGC) rotation creates frequency difference between the WGC mode, we found that the mechanical resonator (MR) can be cooled to the ground state when the propagation direction of driving light is opposite to the spin direction of the WGC, but not from the other side, vice versa, so that the nonreciprocal cooling is achieved. By appropriately selecting the system parameters, the heating process can be completely suppressed due to the quantum interference effect. The proposed approach provides a platform for quantum manipulation of macroscopic mechanical devices beyond the resolved sideband limit.

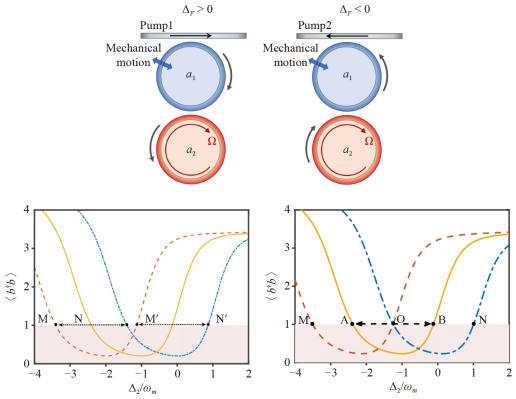

Keywords nonreciprocal ground-state cooling, spinning optomechanical system, optical Sagnac effect

1 Introduction

In recent years, mechanical systems have received increasing attention because they resemble prototypes of classical systems and have become ideal objects for studying the quantum behavior of macroscopic objects [1]. Cavity optomechanics works as an ideal platform to study the quantum properties of macroscopic mechanical systems [2, 3]. However, revealing the quantum effects of mechanical resonators requires strong suppression of uncontrollable thermal fluctuations. Therefore, cooling the mechanical resonators to the ground state is a prerequisite for their potential applications. A lot of theoretical and experimental studies have been conducted on the ground state cooling of mechanical resonators. Among them, the most famous cooling method is the sideband cooling [4–10], which requires the condition of resolved sideband limit to be fulfilled, i.e., the decay rate of the cavity mode is much less than the mechanical frequency. This is a very strict limitation because the cavity requires a high quality factor and is difficult to implement in most physical systems. As such, considerable efforts have been made in the unresolved sideband regime, in which the decay rates would be larger than the vibrational frequency of the MR and can be achievable with a bad cavity. Some approaches have been proposed such as coupled-cavity systems [11–13], atom-assisted systems [14–17], quadratic optomechanical system [18], multi-mode optomechanical system [19–21], and cavity magnomechanical system [22].

Meanwhile, nonreciprocal devices that make incident light show different optical responses in different directions are indispensable in optical communication and optical signal processing [23–27]. Nonreciprocal optics has become an indispensable tool for a wide range of applications such as noise-free sensing, invisibility cloaking,

Higher Education Press

https://doi.org/10.1007/s11467-022-1202-1

directional invisibility cloaking, and one-way optical communication [28–31]. In experiments, the unidirectional flow of classical information has been demonstrated based on optical nonlinearity [32–34], synthetic materials [35], etc. Recently, significant progress has been achieved in nonreciprocal quantum effects, such as nonreciprocal photon blockade [36–38], nonreciprocal entanglement [39], nonreciprocal phonon laser [40], and nonreciprocal mechanical squeezing [41]. These nonreciprocal quantum effects are significant for a variety of quantum technologies.

As the first key step in preparing mechanical quantum states, cooling MRs has been one of the core research directions in the past decades, then nonreciprocal cooling can be understood as a controllable switch between classical and quantum states. Enlightened by the above works, here we propose an scheme for nonreciprocal ground-state cooling in coupled cavities spinning optomechanical system with directional driving. By analyzing the optical force spectrum and deriving the optimal cooling conditions, we demonstrate that the auxiliary WGC mode in our present system brings out the quantum interference effect, so the cooling of MR can be achieved even if the optomechanical cavity decay is in unresolved sideband regime. Meanwhile the optical Sagnac effect generated by the WGC rotation creates a frequency difference between the WGC mode with respect to the directional driving field, we found that the MR can be cooled to the ground state for driving from the opposite direction to the spinning direction of the WGC, but it cannot be cooled effectively from along the spinning direction, vice versa, so that the nonreciprocal cooling is achieved. Compared with the work [11] only considering the coupled cavity without the spin of the cavities, the current scheme has unique advantages. The cooling or heating process is very sensitive to the the optical Sagnac–Fizeau shift which is related to the spinning speed, driving direction. Therefore, it provides the possibility of high controllability and tunability. This opens up a new route for applications in chiral acoustic engineering and the phonon-based information processing and communication.

This paper is organized as follows. In Section 2, the spinning optomechanical system is introduced and the effective Hamiltonian is given. In Section 3, by using the quantum noise approach, we calculate the noise spectrum, and the optimum cooling conditions are obtained. In Section 4, nonreciprocal cooling dynamics of the system is investigated by using master equation. Finally, a brief summary of our work is presented in Section 5.

2 Model and Hamiltonian

We consider a compound optomechanical system as illustrated in Fig. 1, which consisting of an optomechanical anharmonic resonator (with frequency ω_1 and decay rate κ_1 for cavity mode a_1 and frequency ω_m and decay rate γ_m for MR b) and a spinning optical harmonic resonator a_2 (with frequency ω_2 and decay rate κ_2). These two WGC resonators are evanescently coupled to each other with a coupling strength of J [42]. An external laser is coupled into and out of the optical mode a_1 through tapered fibers of frequency ω_d and amplitude ε. For the WGC mode a_2 spinning at angular speed Ω, the light propagates against or along the spinning direction of the WGC a_2 experiences a Fizeau shift Δ_F [43, 44], i.e., $\omega_1 \to \omega_1 + \Delta_F$, with $\Delta_F = \pm\frac{nr\Omega\omega_1}{c}(1 - \frac{1}{n^2} - \frac{\lambda}{n}\frac{\mathrm{d}n}{\mathrm{d}\lambda})$, where $\omega_1 = 2\pi c/\lambda$ is the optical resonance frequency of the nonspinning WGC mode, $c(\lambda)$ is the speed (wavelength) of light in vacuum, n is the refractive index of the cavities. Typically, the dispersion term $\mathrm{d}n/\mathrm{d}\lambda$ describing the relativistic origin of the Sagnac effect is relatively small $\sim 1\%$ [45]. For convenience, we always assume that the WGC mode a_2 rotates clockwise, hence $\pm\Delta_F$ denote light propagating against $(\Delta_F > 0)$ and along $(\Delta_F < 0)$ the direction of the WGC mode, respectively.

In a rotating framework with respect to driving frequencies ω_d, i.e., rotating operator $U = \exp[-\mathrm{i}\omega_d(a_1^\dagger a_1 + a_2^\dagger a_2)]$, the Hamiltonian can be written as

$$\begin{aligned} H_0 =& \Delta_1 a_1^\dagger a_1 + (\Delta_2 + \Delta_F) a_2^\dagger a_2 + \omega_m b^\dagger b \\ &+ g a_1^\dagger a_1 (b^\dagger + b) + J(a_1^\dagger a_2 + a_2^\dagger a_1) + \varepsilon(a_1^\dagger + a_1), \end{aligned} \tag{1}$$

where $\Delta_i = \omega_i - \omega_d$ $(i = 1, 2)$ is the detuning between optical modes and the driving field. Here a (b) is the annihilation operator of the optical modes (MR). We consider a weak optomechanical coupling strength $(g \approx 0.1\omega_m)$ that is well within the current experimental abilities [46–48]. To

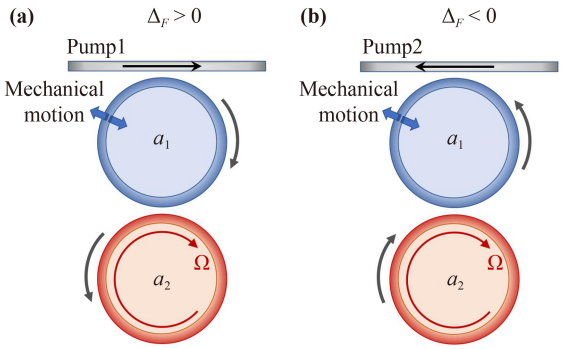

Fig. 1 Schematic diagram of the model. A mechanical mode is coupled to optomechanical cavity a_1 which is driven by a external laser through tapered fibers. Cavity a_2 with clockwise spinning angular speed Ω coupled to cavity a_1. The spinning WGC mode results in different Fizeau drag Δ_F for the different input direction of the driving laser. **(a)** and **(b)** show the driving laser propagating against (along) the direction of the spinning cavity a_2, i.e., $\Delta_F > 0$ $(\Delta_F < 0)$.

obtain the linearized Hamiltonian, the three modes are split into an average amplitude and a fluctuation term, i.e., $a_1 \to \alpha_1 + \delta a_1, a_2 \to \alpha_2 + \delta a_2, b \to \beta + \delta b$, where α_1, α_2 and β denote the steady-state displacements of the optical and mechanical modes. One can then obtain the effective linearized Hamiltonian of the fluctuation operator (for simplicity, hereafter we drop the notation "δ" for all fluctuation operators, as "$\delta a_1 \to a_1$"):

$$\begin{aligned} H_{\text{eff}} =& \Delta_1' a_1^\dagger a_1 + (\Delta_2 + \Delta_F) a_2^\dagger a_2 + \omega_m b^\dagger b \\ &+ G(a_1^\dagger + a_1)(b + b^\dagger) + J(a_1^\dagger a_2 + a_2^\dagger a_1), \end{aligned} \tag{2}$$

where $\Delta_1' = \Delta_1 - g(\beta + \beta^*)$ is the effective detuning of cavity 1, $G = g\alpha_1$ is the enhanced effective optomechanical coupling coefficients.

3 Quantum noise approach

Quantum noise approach permits us to solve the model and gain insight into the cooling results. We can employ the noise spectrum of optical force, which is related to the cooling (heating) coefficient and can also reflect the sensitivity of the weak force measurement [49, 50], defined as $S_{\text{FF}}(\omega) = \int \mathrm{d}t \mathrm{e}^{\mathrm{i}\omega t} \langle F(t)F(0)\rangle$ with the optical force acting on the mechanical motion $F = -G(a_1 + a_1^\dagger)/x_{\text{ZPF}}$, where x_{ZPF} is the zero-point fluctuation. To obtain the absorption spectrum, we transform Langevin equation to frequency domain for facilitate the calculation, meanwhile in the weak coupling regime, the back action of the MR can be ignored. We write the optical Hamiltonian

$$H_{\text{op}} = \Delta_1' a_1^\dagger a_1 + (\Delta_2 + \Delta_F) a_2^\dagger a_2 + J\left(a_1^\dagger a_2 + a_1 a_2^\dagger\right), \tag{3}$$

and the Langevin equations as follows:

$$\begin{aligned} -\mathrm{i}\omega a_1(\omega) =& -(\mathrm{i}\Delta_1' + \kappa_1) a_1(\omega) - \mathrm{i}J a_2(\omega) \\ &- \sqrt{2\kappa_1} a_{1,in}(\omega), \\ -\mathrm{i}\omega a_2(\omega) =& -[\mathrm{i}(\Delta_2 + \Delta_F) + \kappa_2] a_2(\omega) - \mathrm{i}J a_1(\omega) \\ &- \sqrt{2\kappa_2} a_{2,in}(\omega), \end{aligned} \tag{4}$$

where $a_{o,in}$, $o = 1, 2$, are the noise operators associated with the intrinsic cavity dissipation. The correlations for these noise operators are given by

$$\langle a_{o,in}(t) a_{o,in}^\dagger(t')\rangle = \delta(t - t'), \quad \langle a_{o,in}^\dagger(t) a_{o,in}(t')\rangle = 0. \tag{5}$$

As a result, we obtain

$$S_{\text{FF}}(\omega) = \frac{G^2}{x_{\text{ZPF}}^2}[\chi(\omega) + \chi^*(\omega)], \tag{6}$$

where

$$\begin{aligned} \chi_{a_1(\omega)} &= \frac{1}{-\mathrm{i}(\omega - \Delta_1') + \kappa_1}, \\ \chi_{a_2}(\omega) &= \frac{1}{-\mathrm{i}[\omega - (\Delta_2 + \Delta_F)] + \kappa_2}, \\ \chi(\omega) &= \frac{1}{\frac{1}{\chi_{a_1(\omega)}} + J^2 \chi_{a_2}(\omega)}, \end{aligned} \tag{7}$$

$\chi(\omega)$ is the total response function of the coupled cavities; $\chi_{a_1(\omega)}$ and $\chi_{a_2(\omega)}$ are the response functions of a_1 and a_2, respectively. $A_\mp = x_{\text{ZPF}}^2 S_{\text{FF}}(\pm\omega_m)$ stand for the cooling rate A_- and heating rate A_+ for the MR, which mainly determine the final cooling result of the MR. Therefore, in order to obtain the optimal cooling effect, it is necessary to investigate the dependence of the optical force spectrum on the parameters, that is, the effect of the coupling strength between the two cavities J and the effective detuning of the two cavities on $S_{\text{FF}}(\omega)$.

Due to the involvement of the auxiliary cavity a_2, we first investigate the effect of the coupling strength of the two cavities J on the optical force spectrum in order to obtain the optimal value. The optical force spectrum $S_{\text{FF}}(\omega)$ are plotted versus the frequency ω with different optical coupled strength J in Fig. 2. For the case of standard optomechanical system, i.e., $J = 0$, it is necessary to meet the condition of resolved sideband ($\kappa_1 < \omega_m$) to realize ground-state cooling according to the sideband cooling regime [51]. Since our scheme works in the unresolved-sideband regime ($\kappa_1 > \omega_m$), the optical force spectrum will show a Lorentzian line with the width larger than the MR's frequency (gray dotted line), and cooling spectrum $S_{\text{FF}}(+\omega_m)$ and heating spectrum $S_{\text{FF}}(-\omega_m)$ are comparable, thus the ground-state cooling of the MR cannot be achieved [10, 51, 52]. However, in our current scheme, because of the coupling of the two cavities, the optical force spectrum $S_{\text{FF}}(\omega)$ has a more complex form than that of the standard optomechanical system. The Lorentz spectrum will be modified to two peaks and a valley. The position of the valley is always located $\omega = -\omega_m$, the positions of the peaks are determined by

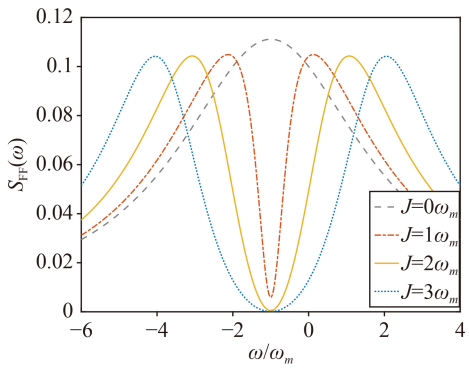

Fig. 2 The optical force spectrum $S_{\text{FF}}(\omega)$ (in arbitrary units) versus the frequency ω for different optical coupled strength J. The parameters are taken as $\Delta_1' = -\omega_m$, $\Delta_2 + \Delta_F = -\omega_m$, $G = 0.1\omega_m$, $\kappa_1 = 3\omega_m$, $\kappa_2 = 0.1\omega_m$.

the value of J. In addition, the width of each peak is smaller than the MR frequency, so that the MR can be cooled close to its ground state even in unresolved sideband case.

Actually, the two split peaks of the optical force spectrum originate precisely from the normal mode splitting due to the coupling between the two cavities. To explain the physical mechanism, we give the diagonalized Hamiltonian $H_{\rm eff}$ with $H_{\rm diag} = E_+ a_b^\dagger a_b + E_- a_d^\dagger a_d + G'(a_b^\dagger + a_b + a_d^\dagger + a_d) \cdot (b^\dagger + b)$, where $a_{b,d} = \frac{a_1 \pm a_2}{\sqrt{2}}$, $G' = \frac{G}{\sqrt{2}}$. By adjusting the appropriate parameters, the MR can resonate with the bright mode, which result in the cooling of the MR. If the MR is far away from resonating, then the MR is decoupled from the diagonalized cavity modes, so the MR will heating by the thermal environment. We give the effective frequency of the normal mode as

$$E_\pm = \frac{1}{2}\left[\Delta_1' + (\Delta_2 + \Delta_F) \pm \sqrt{(\Delta_1' - (\Delta_2 + \Delta_F))^2 + 4J^2}\right]. \tag{8}$$

Here, we focus only on the cooling peak on the right, which corresponds to the optimal cooling effect $E_+ = \omega_m$. Meanwhile, we found that the valley of the optical force spectrum is always located at $\omega = \Delta_2 + \Delta_F = -\omega_m$, in this case, the phenomenon of quantum destructive interference happens, thereby the heating process of MR is suppressed effectively. As a result, we can set

$$J = \sqrt{2\omega_m\,(\omega_m - \Delta_1')}. \tag{9}$$

Optimal cooling is achieved when the above conditions are met.

In Fig. 3, the optical force spectrum $S_{\rm FF}(\omega)$ are plotted versus the frequency ω with different decay rate $\kappa_{1,2}$ under the optimal coupling strength in Eq. (9), where we choose $\Delta_1' = -3\omega_m$, then the corresponding optimal coupling strength $J = 2\sqrt{2}\omega_m$. For the sake of observation, we kept only the valley and the cooling peak on the right. It is worth noting that even if the optimal cooling conditions have been met, the decay rate κ_2 also needs to be controlled, as it directly affects the depth of the valley of heating process, as well as the height of the peak of cooling process. That is, the smaller decay rate κ_2, the better effect for cooling. Moreover, We find that κ_1 does not affect the suppression of the heating process, but does affect the cooling process, but even so, ground-state cooling also can be achieved in the unresolved sideband condition.

4 Nonreciprocal cooling mechanism

The master equation of the system has the following form:

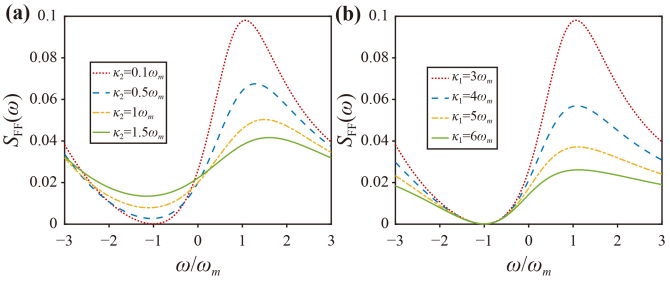

Fig. 3 The optical force spectrum $S_{\rm FF}(\omega)$ (in arbitrary units) versus the frequency ω for different decay rates of **(a)** the second cavity κ_2 and **(b)** the optomechanical cavity κ_1 in the optimum conditions with $\Delta_1' = -3\omega_m$, $J = 2\sqrt{2}\omega_m$, $\Delta_2 + \Delta_F = -\omega_m$, and $G = 0.1\omega_m$. The other parameters are taken as $\kappa_1 = 3\omega_m$ for (a), $\kappa_2 = 0.1\omega_m$ for (b).

$$\dot{\rho} = -\,{\rm i}[H_{\rm eff}, \rho] + \kappa_1 \mathcal{L}[a_1]\rho + \kappa_2 \mathcal{L}[a_2]\rho + \gamma_{\rm m}(n_{\rm th} + 1)\mathcal{L}[b]\rho + \gamma_{\rm m} n_{\rm th} \mathcal{L}\left[b^\dagger\right]\rho, \tag{10}$$

where $\mathcal{L}[o]\rho = o\rho o^\dagger - \left(o^\dagger o\rho + \rho o^\dagger o\right)/2$ is the Lindblad superoperator, describing the decay of the two cavity modes and the mechanical oscillator respectively. $n_{\rm th}$ is the thermal phonon number given by $n_{\rm th} = \left[{\rm e}^{\hbar\omega_{\rm m}/(k_{\rm B}T)} - 1\right]^{-1}$, where T is the environmental temperature and $k_{\rm B}$ is Boltzmann constant.

After discussing the cooling process and the optimal conditions for achieving cooling, we next investigated the nonreciprocal cooling mechanism. Using experimentally feasible parameters [2, 45, 53, 54], that is, $\lambda = 1550$ nm, $n = 1.48$, $r = 4.75$ mm, $\Omega = 6$ kHz and $\omega_m/(2\pi) = 2.3$ MHz, thus $\Delta_F \approx \omega_m$. The resonator with a radius of $r = 1.1$ mm can spin at an angular velocity of $\Omega = 6.6$ kHz [45]. It has been experimentally demonstrated that using a levitated optomechanical system, Ω can even be increased to GHz values [55, 56]. The optomechanical strength g is typically 10^3–10^6 Hz in optical microresonators [2, 46, 57, 58], and J can be adjusted by changing the distance of the double resonators [59]. Figure 4 shows the analytical net cooling rate $\Gamma_{\rm opt} = A_- - A_+$ as a function of the detuning Δ_2, where the yellow curve represents the spin angular velocity of WGC is 0, and the red dashed line (blue dot-dashed line) refers to the laser driven against (along) the spinning direction of a_2, i.e., $\Delta_F > 0$ ($\Delta_F < 0$). It can be seen that the maximum net cooling rate is located at the point $\Delta_2 + \Delta_F = -\omega_m$. The numerical simulation steady-state average phonon number $\langle b^\dagger b\rangle$ versus the effective detuning Δ_2 by using the master equation (10) for $\Delta_F >, =, < 0$ are plotted in Fig. 5. The maximum value of the net cooling rate corresponds exactly to the lowest point of the average phonon number. In Fig. 5(a), there are two nonreciprocal cooling segments on Δ_2-axis, corresponding to horizontal lines MN and M′N′. When the optimal conditions (9) are met, taking the value of Δ_2 from line MN (M′N′), it is possible to obtain the ground-state cooling and get its optimal value near $\Delta_2 + \Delta_F = -\omega_m$ for $\Delta_F > 0$ ($\Delta_F < 0$).

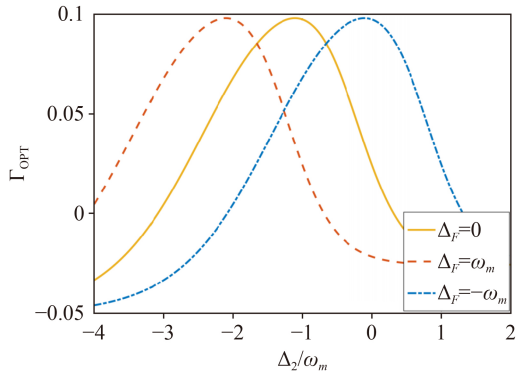

Fig. 4 The net cooling rate $\Gamma_{\rm opt} = A_- - A_+$ versus the detuning of the WGC mode a_2. The yellow solid line represents the spin angular velocity of WGC is 0, and the red dashed line (blue dot-dashed line) refers to the laser driven against (along) the spinning direction of a_2, i.e., $\Delta_F = \omega_m$ ($\Delta_F = -\omega_m$). The parameters are chosen as $\Delta_1' = -3\omega_m$, $J = 2\sqrt{2}\omega_m$, $G = 0.1\omega_m$, $\kappa_1 = 3\omega_m$ and $\kappa_2 = 0.1\omega_m$.

That is say, at a given angular velocity, when the propagation direction of driving light is opposite to the spin direction of a_2, the MR can be cooled down to its ground state, meanwhile the propagation direction of driving light is along with the spin direction of a_2, it cannot be effectively cooled, and vice versa, i.e., nonreciprocal cooling is achieved. The two nonreciprocal cooling segments are separated by $\mathrm{N} \to \mathrm{M}'$, and when the spin angular velocity $\Omega = 0$, the nonreciprocity disappears, even if the direction of the driving laser is changed. In Fig. 5(b), we show that by choosing a special value of Δ_F, we can achieve a maximum range of nonreciprocal cooling regions. In the absence of rotation, points A and B are the two boundary points for the ground-state cooling, respectively. In order to achieve the maximum range of nonreciprocal ground-state cooling, it is essential to make $\Delta_2(B) - \Delta_2(A) = |2\Delta_F|$. Then, the two nonreciprocal segments will intersect at a point O, and $\Delta_2(B) - \Delta_2(O) = \Delta_2(O) - \Delta_2(A) = |\Delta_F|$, the nonreciprocal cooling segment is concentrated in

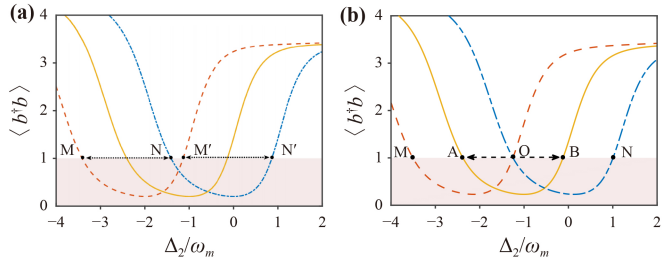

Fig. 5 The steady-state average phonon number $\langle b^\dagger b \rangle$ versus the detuning of the WGC mode a_2. The yellow solid line represents the spin angular velocity of WGC is 0, and the red dashed line (blue dot-dashed line) refers to the laser driven against (along) the spinning direction of a_2. In **(a)**, we choose $\Delta_F = \pm\omega_m$. In **(b)**, we choose $\Delta_F \approx \pm 1.129\omega_m$. Other parameters are the same as Fig. 4, and $n_{\rm th} = 1000$, $\gamma_m = 10^{-5}\omega_m$.

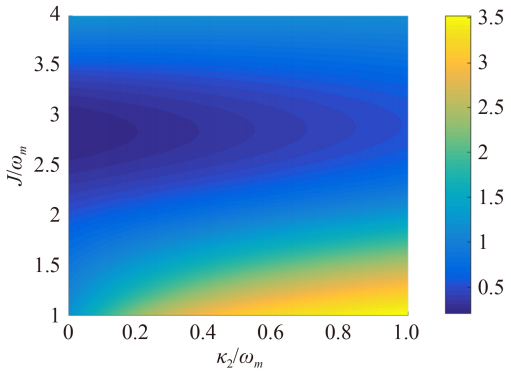

Fig. 6 The average phonon number $\langle b^\dagger b \rangle$ versus the decay rate κ_2 and the optical coupling strength J. The parameters are taken as $\Delta_2 + \Delta_F = -\omega_m$, $n_{\rm th} = 1000$, $\gamma_m = 10^{-5}\omega_m$. Other parameters are the same as Fig. 4.

horizontal line MN.

By employing the master equation, the numerical simulation for the average phonon number $\langle b^\dagger b \rangle$ of the steady state versus the coupled strength of two optical cavities J and the decay rate of WGC mode κ_2 are shown in Fig. 6(a). From the figure, it can be seen that when a value of detuning $\Delta_1 = -3\omega_m$ is given, the optimal cooling can be achieved with the hopping strength between the two cavities at $2\sqrt{2}\omega_m$, which is in accordance with the optimal conditions derived above. In addition, the final average phonon number decreases as the decay rate κ_2 increases.

In Fig. 7(a), $\langle b^\dagger b \rangle$ is plotted versus the optomechanical coupling strength G. We found that the average phonon number decreases with the increase of the optomechanical coupling strength in a appropriate range. This is due to the fact that as the optomechanical coupling strength increases, beam-splitter interaction dominates so the ability of the optical field vacuum bath to absorb thermal phonons increases. When the G continues to increase, the counter rotating-wave term which has a heating effect on the MR gradually dominates, so that the average phonon number tends to increase. In Fig. 7(b), $\langle b^\dagger b \rangle$ is

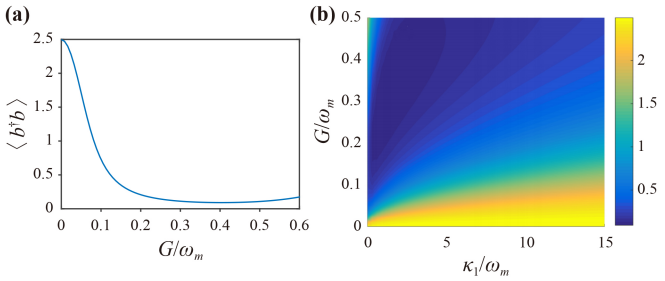

Fig. 7 **(a)** The steady-state average phonon number $\langle b^\dagger b \rangle$ versus the optomechanical coupling strength G. **(b)** The average phonon number $\langle b^\dagger b \rangle$ versus the decay rate κ_1 and the optomechanical coupling strength G. The parameters are taken as $\Delta_2 + \Delta_F = -\omega_m$, $n_{\rm th} = 1000$, $\gamma_m = 10^{-5}\omega_m$. Other parameters are the same as Fig. 4.

shown as a function of the optomechanical coupling strength G and the decay rate κ_1. The average phonon number decreases rapidly as G increases in the appropriate range. Also it gets larger as the decay rate κ_1 increases. It is worth noting that there is a small area in the upper left corner where the average phonon number becomes larger when κ_1 approaches 0. Actually, the vacuum bath of the cavity field extracts the thermal excitation in the MR by means of nonequilibrium dynamics, and then the whole system reaches a steady state. When the optomechanical decay rate κ_1 is approximately 0, the vacuum bath cannot extract the thermal phonons in the MR, so that the system will be thermalized to the thermal equilibrium state.

5 Conclusions

In summary, we theoretically investigate the role of rotation in achieving nonreciprocal ground-state cooling of MR in a system consisting of a cavity optomechanical resonator coupled to a spinning optical resonator. We analyze the optical force spectrum and derive the optimal cooling conditions, and we demonstrate that the auxiliary WGC mode in our present system results in the quantum interference effect, so the cooling of MR can be achieved even if the optomechanical cavity decay is in unresolved sideband regime. We also show that the optical Sagnac effect strongly modifies the cooling and heating process which depending on whether the input direction of the drive laser is opposite to or the same as the direction of the WGC mode. We point out that the mechanical mode coupled to a WGC optical mode has been investigated experimentally [53, 60, 61], in addition, some studies have extended the optical Sagnac effect [38, 40, 44]. The present scheme continues the study of this topic and focuses on the quantum aspects of its nonreciprocal properties.

Acknowledgements This work was supported by the National Natural Science Foundation of China (Grant No. 11874099) and the National Key R&D Program of China (No. 2021YFE0193500).

References

1. M. Poot and H. S. van der Zant, Mechanical systems in the quantum regime, *Phys. Rep.* 511(5), 273 (2012)
2. M. Aspelmeyer, T. J. Kippenberg, and F. Marquardt, Cavity optomechanics, *Rev. Mod. Phys.* 86(4), 1391 (2014)
3. K. y. Zhang, L. Zhou, G. Dong, and W. Zhang, Cavity optomechanics with cold atomic gas, *Front. Phys.* 6(3), 237 (2011)
4. T. Carmon, H. Rokhsari, L. Yang, T. J. Kippenberg, and K. J. Vahala, Temporal behavior of radiation-pressure-induced vibrations of an optical microcavity phonon mode, *Phys. Rev. Lett.* 94(22), 223902 (2005)
5. T. J. Kippenberg, H. Rokhsari, T. Carmon, A. Scherer, and K. J. Vahala, Analysis of radiation-pressure induced mechanical oscillation of an optical microcavity, *Phys. Rev. Lett.* 95(3), 033901 (2005)
6. Y. C. Liu and Y. F. Xiao, Macroscopic mechanical systems are entering the quantum world, *Natl. Sci. Rev.* 2(1), 9 (2015)
7. A. Schliesser, R. Riviere, G. Anetsberger, O. Arcizet, and T. J. Kippenberg, Resolved-sideband cooling of a micromechanical oscillator, *Nat. Phys.* 4(5), 415 (2008)
8. J. D. Teufel, T. Donner, D. Li, J. W. Harlow, M. Allman, K. Cicak, A. J. Sirois, J. D. Whittaker, K. W. Lehnert, and R. W. Simmonds, Sideband cooling of micromechanical motion to the quantum ground state, *Nature* 475(7356), 359 (2011)
9. T. J. Kippenberg and K. J. Vahala, Cavity optomechanics: Back-action at the mesoscale, *Science* 321(5893), 1172 (2008)
10. Y. C. Liu, Y. W. Hu, C. W. Wong, and Y. F. Xiao, Review of cavity optomechanical cooling, *Chin. Phys. B* 22(11), 114213 (2013)
11. Y. Guo, K. Li, W. Nie, and Y. Li, Electromagnetically-induced-transparency-like ground-state cooling in a double-cavity optomechanical system, *Phys. Rev. A* 90(5), 053841 (2014)
12. Y. C. Liu, Y. F. Xiao, X. Luan, Q. Gong, and C. W. Wong, Coupled cavities for motional ground-state cooling and strong optomechanical coupling, *Phys. Rev. A* 91(3), 033818 (2015)
13. W. Gu and G. Li, Quantum interference effects on ground-state optomechanical cooling, *Phys. Rev. A* 87(2), 025804 (2013)
14. S. Zhang, J. Q. Zhang, J. Zhang, C. W. Wu, W. Wu, and P. X. Chen, Ground state cooling of an optomechanical resonator assisted by a Λ-type atom, *Opt. Express* 22(23), 28118 (2014)
15. C. Genes, H. Ritsch, and D. Vitali, Micromechanical oscillator ground-state cooling via resonant intracavity optical gain or absorption, *Phys. Rev. A* 80(6), 061803 (2009)
16. B. Vogell, K. Stannigel, P. Zoller, K. Hammerer, M. T. Rakher, M. Korppi, A. Jöckel, and P. Treutlein, Cavity-enhanced long-distance coupling of an atomic ensemble to a micromechanical membrane, *Phys. Rev. A* 87(2), 023816 (2013)
17. X. Chen, Y. C. Liu, P. Peng, Y. Zhi, and Y. F. Xiao, Cooling of macroscopic mechanical resonators in hybrid atom-optomechanical systems, *Phys. Rev. A* 92(3), 033841 (2015)
18. J. Y. Yang, D. Y. Wang, C. H. Bai, S. Y. Guan, X. Y. Gao, A. D. Zhu, and H. F. Wang, Ground-state cooling of mechanical oscillator via quadratic optomechanical coupling with two coupled optical cavities, *Opt. Express* 27(16), 22855 (2019)
19. C. Genes, D. Vitali, and P. Tombesi, Simultaneous cooling and entanglement of mechanical modes of a micromirror in an optical cavity, *New J. Phys.* 10(9), 095009 (2008)
20. Z. Yang, C. Zhao, R. Peng, S. L. Chao, J. Yang, and L. Zhou, The simultaneous ground-state cooling and synchronization of two mechanical oscillators by driving

nonlinear medium, *Ann. Phys.* 534(5), 2100494 (2022)
21. D. G. Lai, J. F. Huang, X. L. Yin, B. P. Hou, W. Li, D. Vitali, F. Nori, and J. Q. Liao, Nonreciprocal ground-state cooling of multiple mechanical resonators, *Phys. Rev. A* 102(1), 011502 (2020)
22. Z. X. Yang, L. Wang, Y. M. Liu, D. Y. Wang, C. H. Bai, S. Zhang, and H. F. Wang, Ground state cooling of magnomechanical resonator in *PT*-symmetric cavity magnomechanical system at room temperature, *Front. Phys.* 15(5), 52504 (2020)
23. L. Bi, J. Hu, P. Jiang, D. H. Kim, G. F. Dionne, L. C. Kimerling, and C. Ross, On-chip optical isolation in monolithically integrated non-reciprocal optical resonators, *Nat. Photonics* 5(12), 758 (2011)
24. R. J. Potton, Reciprocity in optics, *Rep. Prog. Phys.* 67(5), 717 (2004)
25. P. Lodahl, S. Mahmoodian, S. Stobbe, A. Rauschenbeutel, P. Schneeweiss, J. Volz, H. Pichler, and P. Zoller, Chiral quantum optics, *Nature* 541(7638), 473 (2017)
26. X. W. Xu, H. Q. Shi, and A. X. Chen, Nonreciprocal transition between two indirectly coupled energy levels, *Front. Phys.* 17(4), 42505 (2022)
27. X. B. Yan, H. L. Lu, F. Gao, and L. Yang, Perfect optical nonreciprocity in a double-cavity optomechanical system, *Front. Phys.* 14(5), 52601 (2019)
28. Z. Lin, H. Ramezani, T. Eichelkraut, T. Kottos, H. Cao, and D. N. Christodoulides, Unidirectional invisibility induced by *PT*-symmetric periodic structures, *Phys. Rev. Lett.* 106(21), 213901 (2011)
29. M. A. Miri, F. Ruesink, E. Verhagen, and A. Alù, Optical nonreciprocity based on optomechanical coupling, *Phys. Rev. Appl.* 7(6), 064014 (2017)
30. L. Feng, M. Ayache, J. Huang, Y. L. Xu, M. H. Lu, Y. F. Chen, Y. Fainman, and A. Scherer, Nonreciprocal light propagation in a silicon photonic circuit, *Science* 333(6043), 729 (2011)
31. M. Scheucher, A. Hilico, E. Will, J. Volz, and A. Rauschenbeutel, Quantum optical circulator controlled by a single chirally coupled atom, *Science* 354(6319), 1577 (2016)
32. B. Peng, Ş. K. Özdemir, F. Lei, F. Monifi, M. Gianfreda, G. L. Long, S. Fan, F. Nori, C. M. Bender, and L. Yang, Parity–time-symmetric whispering-gallery microcavities, *Nat. Phys.* 10(5), 394 (2014)
33. H. Xiong, L. G. Si, X. Yang, and Y. Wu, Asymmetric optical transmission in an optomechanical array, *Appl. Phys. Lett.* 107(9), 091116 (2015)
34. J. Kim, M. C. Kuzyk, K. Han, H. Wang, and G. Bahl, Non-reciprocal Brillouin scattering induced transparency, *Nat. Phys.* 11(3), 275 (2015)
35. S. Barzanjeh, M. Wulf, M. Peruzzo, M. Kalaee, P. Dieterle, O. Painter, and J. M. Fink, Mechanical on-chip microwave circulator, *Nat. Commun.* 8(1), 953 (2017)
36. R. Huang, A. Miranowicz, J. Q. Liao, F. Nori, and H. Jing, Nonreciprocal photon blockade, *Phys. Rev. Lett.* 121(15), 153601 (2018)
37. K. Wang, Q. Wu, Y. F. Yu, and Z. M. Zhang, Nonreciprocal photon blockade in a two-mode cavity with a second-order nonlinearity, *Phys. Rev. A* 100(5), 053832 (2019)
38. B. Li, R. Huang, X. Xu, A. Miranowicz, and H. Jing, Nonreciprocal unconventional photon blockade in a spinning optomechanical system, *Photon. Res.* 7(6), 630 (2019)
39. Y. F. Jiao, S. D. Zhang, Y. L. Zhang, A. Miranowicz, L. M. Kuang, and H. Jing, Nonreciprocal optomechanical entanglement against backscattering losses, *Phys. Rev. Lett.* 125(14), 143605 (2020)
40. Y. Jiang, S. Maayani, T. Carmon, F. Nori, and H. Jing, Nonreciprocal phonon laser, *Phys. Rev. Appl.* 10(6), 064037 (2018)
41. S. S. Chen, S. S. Meng, H. Deng, and G. J. Yang, Nonreciprocal mechanical squeezing in a spinning optomechanical system, *Ann. Phys.* 533(1), 2000343 (2021)
42. S. M. Spillane, T. J. Kippenberg, O. J. Painter, and K. J. Vahala, Ideality in a fiber-taper-coupled microresonator system for application to cavity quantum electrodynamics, *Phys. Rev. Lett.* 91(4), 043902 (2003)
43. G. B. Malykin, The Sagnac effect: Correct and incorrect explanations, *Phys. Uspekhi* 43(12), 1229 (2000)
44. H. Lü, Y. Jiang, Y.-Z. Wang, and H. Jing, Optomechanically induced transparency in a spinning resonator, *Photon. Res.* 5(4), 367 (2017)
45. S. Maayani, R. Dahan, Y. Kligerman, E. Moses, A. U. Hassan, H. Jing, F. Nori, D. N. Christodoulides, and T. Carmon, Flying couplers above spinning resonators generate irreversible refraction, *Nature* 558(7711), 569 (2018)
46. L. Ding, C. Baker, P. Senellart, A. Lemaitre, S. Ducci, G. Leo, and I. Favero, Wavelength-sized GaAs optomechanical resonators with gigahertz frequency, *Appl. Phys. Lett.* 98(11), 113108 (2011)
47. G. Enzian, M. Szczykulska, J. Silver, L. Del Bino, S. Zhang, I. A. Walmsley, P. Del'Haye, and M. R. Vanner, Observation of Brillouin optomechanical strong coupling with an 11 GHz mechanical mode, *Optica* 6(1), 7 (2019)
48. H. Snijders, J. A. Frey, J. Norman, M. P. Bakker, E. C. Langman, A. Gossard, J. E. Bowers, M. P. van Exter, D. Bouwmeester, and W. Löffler, Purification of a single-photon nonlinearity, *Nat. Commun.* 7(1), 12578 (2016)
49. S. L. Chao, Z. Yang, C. S. Zhao, R. Peng, and L. Zhou, Force sensing in a dual-mode optomechanical system with linear–quadratic coupling and modulated photon hopping, *Opt. Lett.* 46(13), 3075 (2021)
50. X. Li, B. Xiong, S. Chao, C. Zhao, H. T. Tan, and L. Zhou, Remote weak-signal measurement via bound states in optomechanical systems, *Commum. Theor. Phys.* 73(2), 025102 (2021)
51. I. Wilson-Rae, N. Nooshi, W. Zwerger, and T. J. Kippenberg, Theory of ground state cooling of a mechanical oscillator using dynamical backaction, *Phys. Rev. Lett.* 99(9), 093901 (2007)
52. F. Marquardt, J. P. Chen, A. A. Clerk, and S. M. Girvin, Quantum theory of cavity-assisted sideband cooling of mechanical motion, *Phys. Rev. Lett.* 99(9), 093902 (2007)
53. K. J. Vahala, Optical microcavities, *Nature* 424(6950), 839 (2003)
54. G. C. Righini, Y. Dumeige, P. Feron, M. Ferrari, G. Nunzi Conti, D. Ristic, and S. Soria, Whispering gallery mode microresonators: Fundamentals and applications,

Riv. Nuovo Cim. 34, 435 (2011)

55. R. Reimann, M. Doderer, E. Hebestreit, R. Diehl, M. Frimmer, D. Windey, F. Tebbenjohanns, and L. Novotny, GHZ rotation of an optically trapped nanoparticle in vacuum, *Phys. Rev. Lett.* 121(3), 033602 (2018)
56. J. Ahn, Z. Xu, J. Bang, Y. H. Deng, T. M. Hoang, Q. Han, R. M. Ma, and T. Li, Optically levitated nanodumbbell torsion balance and GHz nanomechanical rotor, *Phys. Rev. Lett.* 121(3), 033603 (2018)
57. E. Verhagen, S. Deléglise, S. Weis, A. Schliesser, and T. J. Kippenberg, Quantum-coherent coupling of a mechanical oscillator to an optical cavity mode, *Nature* 482(7383), 63 (2012)
58. Y. Zeng, B. Xiong, and C. Li, Suppressing laser phase noise in an optomechanical system, *Front. Phys.* 17(1), 12503 (2022)
59. J. Zhang, B. Peng, Ş. K. Özdemir, K. Pichler, D. O. Krimer, G. Zhao, F. Nori, Y. Liu, S. Rotter, and L. Yang, A phonon laser operating at an exceptional point, *Nat. Photonics* 12(8), 479 (2018)
60. M. Li, W. Pernice, and H. Tang, Tunable bipolar optical interactions between guided lightwaves, *Nat. Photonics* 3(8), 464 (2009)
61. I. S. Grudinin, H. Lee, O. Painter, and K. J. Vahala, Phonon laser action in a tunable two-level system, *Phys. Rev. Lett.* 104(8), 083901 (2010)